An Ultra Wideband Transmitted Reference Scheme Gaining from Intersymbol Interference

Florian Troesch and Armin Wittneben
Communication Technology Laboratory, ETH Zurich, 8092 Zurich, Switzerland
Email: {troeschf, wittneben}@nari.ee.ethz.ch

***Abstract*— We consider a wireless body area network (WBAN) with an average per link throughput of about 500 kbps based on an ultra wideband (UWB) transmitted reference (TR) scheme. For a long battery autonomy a low duty cycle operation of the nodes and thus a high peak data rate is a promising concept. Due to a moderate path loss, a peak data rate in excess of 50 Mbps would be feasible with respect to the FCC power constraints. With current low complexity UWB TR systems, the peak data rate is constrained to much lower values, because they are sensitive to intersymbol interference (ISI). Therefore, the impact of moderate ISI on symbolwise UWB TR detectors is investigated. It is shown that presented UWB TR scheme is robust to ISI and for a specific system setup even benefits from ISI. Due to this gain, the UWB TR scheme outperforms differential phase shift keying (DPSK) in presence of ISI and the FCC peak power constraint.**

I. Introduction

Ultra wideband (UWB) wireless body area networks (WBAN) gained much interest due to a bunch of attractive applications as wireless health monitoring and ubiquitous computing. Since WBAN nodes get their power from rechargeable batteries, it is inevitable that they are extremely energy efficient. To meet such energy requirements, a low duty cycle operation of the nodes and thus a high peak data rate are essential. Due to a moderate path loss in WBANs [1], a peak data rate in excess of 50 Mbps would be feasible within the FCC power constraints for UWB systems. But the peak data rate is constrained to much lower values with current low complexity systems, such as UWB transmitted reference (TR) systems, as they are sensitive to intersymbol interference (ISI).

The impact of ISI on UWB TR was already addressed in different publications. However, often ISI mitigation techniques are proposed which require over-sampling, complex digital signal processing, or sequence estimation, leading to too complex receivers for considered WBAN applications [2]–[4].

We focus on very basic UWB TR systems with symbolwise detection. Each bit is represented by a modulated data pulse and an unmodulated and delayed reference pulse. Due to a very low duty cycle operation of the system a multiple access scheme is realized by a time-division multiple access (TDMA) approach or omitted entirely. The impact of moderate ISI is investigated with respect to different system parameters such as data rate, TR delay between data and reference pulse as well as integration interval. This is done based on bit error rate (BER) considerations. It is shown that with moderate ISI of at most one half-frame, the UWB TR receiver can avoid ISI effects at the expense of a reduced receive signal power. Furthermore, it is demonstrated that by setting the TR delay equal to half the symbol period, it is possible to avoid ISI at the receiver without any loss in signal power. Even a reduction in noise power compared to the no ISI case is achieved. This is possible as the specific ISI structure allows the receiver to collect the entire signal energy while integrating over a shorter duration. This gain leads to advantages of UWB TR over differential phase shift keying (DPSK) systems in presence of ISI and the FCC peak power constraint [5].

The paper is organized as follows. After the introduction of the discrete system model in the following section, a BER analysis for three different scenarios is presented in Section III. In Section IV, TR performance results are presented and compared to binary pulse position modulation with energy detection (BPPM-ED) as well as to DPSK.

II. Discrete System Model

A. Transmitted Reference

A real discrete time system model of considered UWB TR system is shown in Fig. 1. It is assumed that only two pulses per bit are transmitted with considered TR scheme or one pulse per bit with BPPM-ED and with DPSK. This is reasonable for short range communication due to a moderate path loss [1]. A multiple access scheme is omitted. The frame length is determined by $N = 2B/R$, where B is the system bandwidth and R is the data rate. The factor 2 arises because the consider system model is real. We focus on indoor environments, where the channel impulse response (CIR) stays constant over at least one burst of pulses, which justifies a block fading model. Hence, the receive signal $r[k]$ is characterized by the transmitted signal $s[k]$ distorted by the channel $h[k]$ and additive white Gaussian noise $n[k]$. Each frame contains two transmit pulses. One pulse at the beginning of the frame and one delayed by D samples. One pulse is modulated by $a_s \in \{-1, 1\}$ and the other serves as reference pulse. Two different TR schemes are considered which differ in their order of data and reference pulse. With the traditional TR scheme (TR-T) which is considered in most publications on UWB TR, the first pulse severs as reference pulse, i.e., as pilot, while the second one is modulated. It will be shown that under certain circumstances, it is strongly advantageous to first transmit the modulated pulse and then the reference pulse. We refer to this scheme as TR reversed (TR-R).

We map the s-th symbol a_s, to the vector $\vec{x}_s$ according to

$$a_s = -1 \rightarrow \vec{x}_s = [x_{2s}, x_{2s+1}]^T = [-1, 1]^T \quad (1)$$
$$a_s = 1 \rightarrow \vec{x}_s = [x_{2s}, x_{2s+1}]^T = [1, 1]^T, \quad (2)$$

for TR-T and

$$a_s = -1 \rightarrow \vec{x}_s = [x_{2s}, x_{2s+1}]^T = [1, -1]^T \quad (3)$$
$$a_s = 1 \rightarrow \vec{x}_s = [x_{2s}, x_{2s+1}]^T = [1, 1]^T, \quad (4)$$

for TR-R. With this the received signal is described as:

$$r[k] = \sum_s \sqrt{E_b/2}\; x_{2s} h\left[k - sN\right] + \sqrt{E_b/2}\; x_{2s+1} h\left[k - sN - D\right] + n\left[k\right] \quad (5)$$

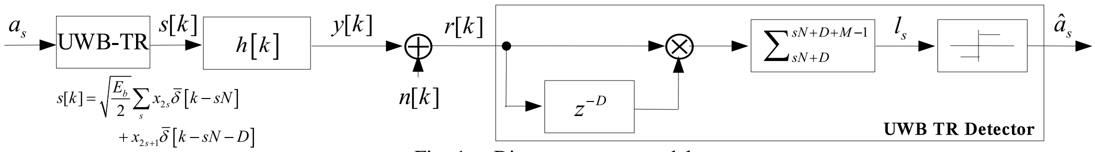

Fig. 1. Discrete system model

where $h[k]$ and $n[k]$ correspond to the k-th sample of the discrete CIR and the additive Gaussian noise, respectively. Due to moderate ISI, the length L of the discrete CIR is limited to $L \leq N$. For convenience, we introduce a vector notation and consider

$$\vec{h} = [h[0], h[1], \dots, h[L-1]]^T \tag{6}$$

as a fixed realization of a discrete CIR consisting of L independently distributed real Gaussian random variables. No path loss is considered and therefore $\mathcal{E}\left\{\|\vec{h}\|^2\right\} = 1$. The noise samples $n[k]$ are realizations of an uncorrelated real discrete Gaussian noise processes with $\mathcal{E}\{n[k]n[k-\nu]\} = \frac{\sigma^2}{2}\bar{\delta}(\nu)$. The TR receiver multiplies the receive signal $r[k]$ with a delayed version $r[k-D]$ and sums over M samples. The output of the integrator corresponding to the s-th decision variable equals:

$$l_s = \vec{r}_{s,0}^T \vec{r}_{s,1}, \tag{7}$$

where

$$\vec{r}_{s,0} = [r[sN], r[sN+1], \dots, r[sN+M-1]]^T \tag{8}$$

$$\vec{r}_{s,1} = [r[sN+D], r[sN+D+1], \dots, r[sN+D+M-1]]^T \tag{9}$$

are the vectors corresponding to delayed and non-delayed part of the receive signal $r[k]$ used for the multiplication. For further derivation, both discrete CIR and noise are grouped according to:

$$\vec{h}_0 = [h[0] \dots, h[M-1]]^T \tag{10}$$

$$\vec{h}_1 = [h[D], \dots, h[D+M-1]]^T \tag{11}$$

and

$$\vec{n}_{s,0} = [n[sN], \dots, n[sN+M-1]]^T \tag{12}$$

$$\vec{n}_{s,1} = [n[sN+D], \dots, n[sN+D+M-1]]^T. \tag{13}$$

B. Binary Pulse Position Modulation with Energy Detection Receiver

Although not focused in this work, BPPM-ED is a promising UWB low complexity, low power approach, too. When normalized to the same energy per bit, BPPM-ED and TR show the same performance in absence of ISI. But in general, the performance of symbolwise BPPM-ED degrades drastically more in presence of ISI than a corresponding TR scheme. This will be shown in Section IV. A low complexity post-detection algorithm based on maximum likelihood sequence estimation (MLSE) has been proposed [6], which significantly improves the performance of a symbolwise ED front-end. We briefly introduce both symbolwise ED and MLSE-ED approach to show their performance plots as benchmark for the TR schemes in Section IV.

With BPPM each frame contains one pulse. Using the notation from the previous section, the s-th BPPM symbol a_s is mapped to the vector $\vec{x}_s$ according to

$$a_s = -1 \rightarrow \vec{x}_s = [x_{2s}, x_{2s+1}]^T = \sqrt{2}[1,0]^T \tag{14}$$

$$a_s = 1 \rightarrow \vec{x}_s = [x_{2s}, x_{2s+1}]^T = \sqrt{2}[0,1]^T, \tag{15}$$

where $D = M = N/2$. The factor $\sqrt{2}$ is introduced to normalize the energy per bit to the same E_b as for TR. The decision variable of the symbolwise ED can now be written as:

$$l_s = \|\vec{r}_{s,1}\|^2 - \|\vec{r}_{s,0}\|^2. \tag{16}$$

Considered MLSE is a simple two state Viterbi algorithm working on the non-linear output samples l_s [6].

C. Differential Phase Shift Keying

Another important low complexity, low power scheme for UWB is DPSK. Instead of retransmitting a reference pulse within each bit, considered DPSK uses the previous data pulse as reference. Hence, only a single pulse per bit is transmitted. This brings major advantages with respect to TR. Both the required energy per bit as well as the ISI occurring at a given data rate is approximately a factor 2 smaller than with TR. All the same, it will be shown that under a FCC peak power constraint TR-R outperforms DPSK.

Using the same notation as above, we have $x_s = a_s x_{s-1}$ with $x_s \in \sqrt{2}\{-1,1\}$ and $a_s \in \{-1,1\}$. The receive signal equals:

$$r[k] = \sqrt{E_\text{b}}\left(\sum_s x_s h[k-sN]\right) + n[k]. \tag{17}$$

and the decision variable after the correlator can be described using the same notation as for (7), leading to

$$l_{s+1} = \vec{r}_{s,0}^T \vec{r}_{s,1}, \tag{18}$$

with $D = N = M$.

III. Performance Analysis

In order to keep the following evaluation readable we set $E_\text{b} = 2$.

A. No ISI

We consider the no ISI case, where the UWB TR system transmits at the highest data rate R possible without ISI. Hence, a bit is transmitted every $N = 2L$. In the absence of noise, a part of a possible receive signal is shown in Fig. 2 for $a_{s-1} = a_s = 1$. The

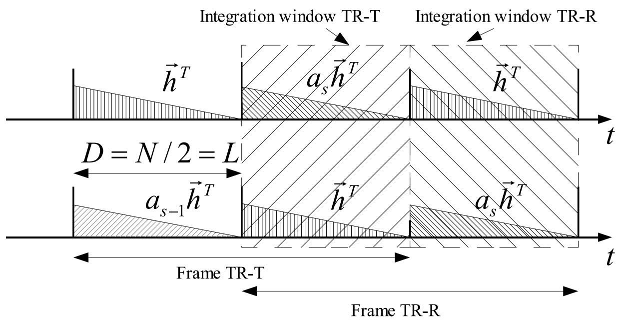

Fig. 2. Signal example of non-delayed and delayed correlation input in absence of ISI with $N/2 = L$.

TR receiver multiplies the received signal (upper part) with a copied version of the receive signal (lower part), which has been delayed by $D = N/2$ samples. For both TR-T and TR-R, frame and integration period are indicated. Setting the integration duration $M = D$, the receiver integrates over the whole second half of the s-th frame to obtain the decision variable for the s-th symbol. From Fig. 2, it is apparent that the TR-R scheme can also be realized by changing the integration period of the TR-T scheme instead of changing the pulse order, but in this case the first pulse is lost. In absence of ISI, TR-T and TR-R work on the same decision statistics and therefore show the same performance. Therefore, the following BER analysis is with respect to TR-T only:

$$\begin{aligned} l_s &= \left(\vec{h} + \vec{n}_{s,0}\right)^T \left(a_s\vec{h} + \vec{n}_{s,1}\right) && (19)\\ &= a_s\|h\|^2 + a_s\vec{n}_{s,0}^T\vec{h} + \vec{h}^T\vec{n}_{s,1} + \vec{n}_{s,0}^T\vec{n}_{s,1} && (20)\\ &= \nu_s + \xi_s + \zeta_s, && (21)\end{aligned}$$

where ν_s is the signal component, ξ_s the linear and ζ_s the non-linear noise term corresponding to the s-th symbol. Both ξ_s and ζ_s are zero-mean with variances:

$$\begin{aligned} \sigma_{\xi,s}^2 &= 2\|\vec{h}\|^2\frac{\sigma^2}{2} = \|\vec{h}\|^2\sigma^2 && (22)\\ \sigma_{\zeta,s}^2 &= L\left(\frac{\sigma^2}{2}\right)^2 = \frac{L\sigma^4}{4}. && (23)\end{aligned}$$

The Central Limit theorem, i.e., the Gaussian approximation of the non-linear noise term and the observation that the correlation between ξ_s and ζ_s is zero, leads to the BER conditioned on the CIR [7]:

$$P_{e|\vec{h}} = \mathcal{Q}\left(\frac{\|\vec{h}\|^2}{\sqrt{\|\vec{h}\|^2\sigma^2 + \frac{L\sigma^4}{4}}}\right). \qquad (24)$$

Fig. 2 shows that in case of $D = N/2 = L$, it could be advantageous to integrate over both the TR-T and the TR-R integration period, although some correlation occurs. This leads to the decision variable:

$$\begin{aligned} l_s &= \left(\vec{h} + \vec{n}_{s,0}\right)^T \left(a_s\vec{h} + \vec{n}_{s,1}\right) + \\ &\quad \left(a_s\vec{h} + \vec{n}_{s,1}\right)^T \left(\vec{h} + \vec{n}_{s+1,0}\right) && (25)\\ &= 2a_s\|\vec{h}\|^2 + \vec{h}^T\vec{n}_{s,1} + a_s\vec{n}_{s,0}^T\vec{h} + \vec{n}_{s,1}^T\vec{h} \\ &\quad + a_s\vec{h}^T\vec{n}_{s+1,0} + \vec{n}_{s,0}^T\vec{n}_{s,1} + \vec{n}_{s,1}^T\vec{n}_{s+1,0}. && (26)\end{aligned}$$

Due to the doubled integration window, the energy of the signal component increases by 6 dB to $4a_s^2\|\vec{h}\|^4$ but also the noise variance increases by more than 3 dB due to correlation between first and second window. Repeating similar evaluation steps as above leads to:

$$P_{e|\vec{h}} = \mathcal{Q}\left(\frac{\|\vec{h}\|^2}{\sqrt{\frac{3}{4}\|\vec{h}\|^2\sigma^2 + \frac{L\sigma^4}{8}}}\right). \qquad (27)$$

Hence, integration over two windows brings a clear improvement and shows that TR-T and TR-R are rather inefficient in case of $D = N/2$. This is only true for $D = N/2$ as otherwise reference and data pulse are not aligned in the first and second slot (see Section IV).

B. Moderate ISI with $D = N/2$

Considering the same maximum excess delay L as for the no ISI case, the data rate of the system is doubled to $\hat{R} = 2R$, which causes moderate ISI due to $N = L$. First, the special case $D = N/2$ is analyzed as evaluation is easier and more intuitive than for the more general case. An example of a receive signal for this case is shown in Fig. 3 with $a_s = a_{s-1} = 1$. Again TR-T and TR-R integration windows are indicated. According to the figure, $\vec{h}$ is split

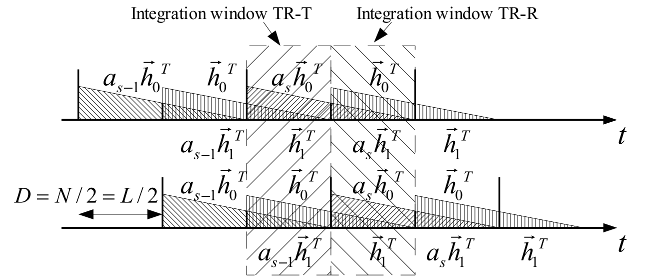

Fig. 3. Signal example of non-delayed and delayed correlation input in presence of moderate ISI with $N = L$ and $D = N/2$.

into two parts, $\vec{h}_0$ and $\vec{h}_1$, of length $L/2$, each. While $\vec{h}_0$ equals the signal part, $\vec{h}_1$ is ISI falling into a subsequent half-frame. The TR-T receiver suffers significantly from ISI, while the TR-R receiver still omits sever ISI effects, by integration over the second half-frame. This effect can be seen by writing down the decision variable for TR-T

$$\begin{aligned} l_s &= \left(\vec{h}_0 + a_{s-1}\vec{h}_1 + \hat{\vec{n}}_{s-1,1}\right)^T \\ &\quad \left(a_s\vec{h}_0 + \vec{h}_1 + \hat{\vec{n}}_{s,0}\right), && (28)\end{aligned}$$

and TR-R

$$\begin{aligned} l_s &= \left(\vec{h}_0 + a_s\vec{h}_1 + \hat{\vec{n}}_{s,1}\right)^T \\ &\quad \left(a_s\vec{h}_0 + \vec{h}_1 + \hat{\vec{n}}_{s,0}\right), && (29)\end{aligned}$$

where $\hat{\vec{n}}_{s-1,1}$, $\hat{\vec{n}}_{s,0}$ and $\hat{\vec{n}}_{s,1}$ all have $L/2$ entries. According to (28), TR-T suffers significantly from the term $a_{s-1}\vec{h}_1$ which correlates perfectly with $\vec{h}_1$. While TR-T suffers from ISI, the lack of a_{-1} in (29) points out that no severe ISI occurs in the decision variable of TR-R. Hence, by integration over the second window, or equivalently using TR-R, ISI can be avoided. Reformulating (29), it appears that this is even achieved without any loss in receive signal power:

$$\begin{aligned} l_s &= a_s\|h\|^2 + 2\vec{h}_0^T\vec{h}_1 + \left(a_s\vec{h}_1 + \vec{h}_0\right)^T \hat{\vec{n}}_{s,0} \\ &\quad + \hat{\vec{n}}_{s,1}^T\left(a_s\vec{h}_0 + \vec{h}_1\right) + \hat{\vec{n}}_{s,1}^T\hat{\vec{n}}_{s,0}. && (30)\end{aligned}$$

The signal energy $\|h\|^2$ is collected by using an integration duration of only $N/2 = L/2$ samples. This leads to a reduced noise variance of the non-linear noise term $\hat{\vec{n}}_{s,1}^T\hat{\vec{n}}_{s,0}$ compared to $\vec{n}_{s,1}^T\vec{n}_{s,0}$ from the no ISI case in (21). This is enabled by the correlation between $a_s\vec{h}_1$ from symbol s and $\vec{h}_1$ from the reference pulse in symbol $s-1$, which extends into symbol s. Applying the Central Limit theorem again leads to the BER conditioned on the CIR:

$$\begin{aligned} P_{e|\vec{h}} &= \frac{1}{2}\left[\mathcal{Q}\left(\frac{\|h\|^2 + 2\vec{h}_0^T\vec{h}_1}{\sqrt{\|h\|^2\sigma^2 + 2\vec{h}_0^T\vec{h}_1\sigma^2 + \frac{L\sigma^4}{8}}}\right)\right. \\ &\quad \left. + \; \mathcal{Q}\left(\frac{\|h\|^2 - 2\vec{h}_0^T\vec{h}_1}{\sqrt{\|h\|^2\sigma^2 - 2\vec{h}_0^T\vec{h}_1\sigma^2 + \frac{L\sigma^4}{8}}}\right)\right]. && (31)\end{aligned}$$

Comparing (31) to (24), the reduced variance in the non-linear noise term is apparent. This gain is achieved at the expense of cross-correlation terms. However according to the Law of Large numbers, the term $2\vec{h}_1^T\vec{h}_0$ vanishes for large L, leading to $P_{e|\vec{h}} = \mathcal{Q}\left(\|\vec{h}\|^2/\sqrt{\|\vec{h}\|^2\sigma^2 + L\sigma^4/8}\right)$ .This shows that for a small cross-correlation, a BER gain can be achieved with respect to the no ISI case, while the data rate is doubled and the TR delay halved. Even with respect to the double window approach, TR-R performs only marginally worse at twice the data rate.

C. Moderate ISI with $D \neq \frac{N}{2}$

In this section, the impact of moderate ISI is discussed for the case, where the delay between data and reference pulse is $D \neq \frac{N}{2}$. The fundamental difference to the case $D = N/2$ is that ISI and signal components are not aligned and therefore, show small correlation. In principle, this means that the impact of interfering components is smaller than with $D = N/2$, and that the performance of TR-R and TR-T approach each other. As a representative example, we focus on TR-T with $D = N/3$. An example of the receive signal for $a_s = a_{s-1} = 1$ is depicted in Fig. 4. As indicated, three different

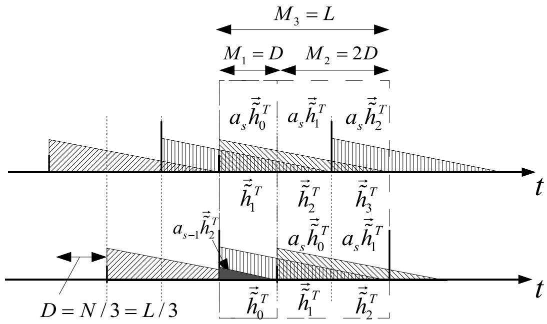

Fig. 4. Signal example of non-delayed and delayed correlation input in presence of moderate ISI with $N = L$ and $D = N/3$.

integration periods M_1, M_2 and M_3 are discussed with different amount of ISI, signal energy and aliasing terms. We group both noise and CIR samples corresponding to the s-th symbol into three vectors according to

$$\vec{\tilde{h}}_i = [h[iN/3], \ldots, h[(i+1)N/3 - 1]]^T \quad (32)$$

$$\vec{\tilde{n}}_{s,i} = [n[sN + iN/3], \ldots, n[sN + (i+1)N/3 - 1]]^T, \quad (33)$$

with $i \in \{0, 1, 2\}$. For all three integration periods aliasing or ISI terms appear, but all are based on cross-correlation terms with zero-mean in average. While the probability of error depends on the instantaneous cross-correlation terms for small L, their impact vanishes for large L due to the Law of Large Numbers. Hence, for large L the impact of ISI and aliasing disappears. The probabilities of error for the three different integration periods equal:

$$P_{e|\vec{h}}^{(M1)} = \mathcal{Q}\left(\frac{\left\|\vec{\tilde{h}}_0\right\|^2}{\sqrt{\left(2\left\|\vec{\tilde{h}}_0\right\|^2 + \left\|\vec{\tilde{h}}_1\right\|^2 + \left\|\vec{\tilde{h}}_2\right\|^2\right)\frac{\sigma^2}{2} + \frac{L\sigma^4}{12}}}\right) \quad (34)$$

$$P_{e|\vec{h}}^{(M2)} = \mathcal{Q}\left(\frac{\left\|\vec{\tilde{h}}_1\right\|^2 + \left\|\vec{\tilde{h}}_2\right\|^2}{\sqrt{\left(4\left\|\vec{\tilde{h}}_0\right\|^2 + 3\left\|\vec{\tilde{h}}_1\right\|^2 + 3\left\|\vec{\tilde{h}}_2\right\|^2\right)\frac{\sigma^2}{2} + \frac{L\sigma^4}{6}}}\right) \quad (35)$$

$$P_{e|\vec{h}}^{(M3)} = \mathcal{Q}\left(\frac{\|\vec{h}\|^2}{\sqrt{6\|\vec{h}\|^2\frac{\sigma^2}{2} + \frac{L\sigma^4}{4}}}\right) \quad (36)$$

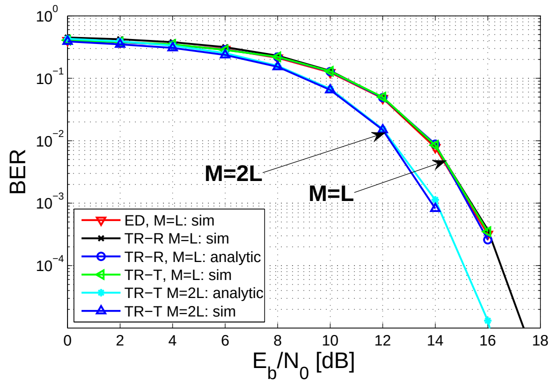

Fig. 5. BER of transmitted reference in absence of ISI with $D = N/2 = L$

According to these equations longer integration periods increase the performance, if sufficient energy can be collected. With a uniform power delay profile with $\|\vec{\tilde{h}}_0\|^2 = \|\vec{\tilde{h}}_1\|^2 = \|\vec{\tilde{h}}_2\|^2 = E$, the probability of error is reduced significantly from $P_{e|\vec{h}}^{(M1)}$ to $P_{e|\vec{h}}^{(M3)}$. It is apparent that there exists an optimal integration period for every average power delay profile and signal-to-noise ratio (SNR).

IV. Performance Results

In this section, BER performance achieved from realistic Monte-Carlo simulations at a rate of 25 Mbps are considered with a frame duration of 40 ns. Lower and upper cut-off frequency of the transmit pulse are $f_l = 3.1$ GHz and $f_u = 6.1$ GHz, respectively. In order to keep the set of variable parameters small, a uniform power delay profile (PDP) is considered. For a given delay spread this corresponds to a worst case situation. The simulated system translates into an equivalent discrete model with $N = 240$ samples per frame.

In Fig. 5, BERs for TR as well as ED are shown in absence of ISI, whereby the maximum excess delay of the channel equals half a frame duration $L = N/2$. If the integration duration is set to half a frame, i.e., $M = N/2 = L$, TR-R, TR-T as well as the ED show all the same performance. This highlights the fact that in absence of ISI, ED, TR-T and TR-R are equivalent with respect to BER performance. Doubling, the integration duration to $M = N$ leads to a performance increase of about 1.5 dB. Hence, the impact of correlated noise terms from the two integration windows is moderate and it is worthwhile to integrate over the whole frame. The good match between analysis and simulation results proves the appropriateness of the Central Limit theorem and the Gaussian approximation for the scenario at hand.

In Fig. 6, the BER performance of TR-T at data rate $\hat{R} = 2R$ with $D = N/3$ and integration periods $M1$ and $M3$ is shown. Both analytic and simulation results are shown. As reference the BER of TR-T at data rate R is plotted. The ED performance with and without MLSE post-detection is added for comparison as well. Due to the lack of any CSI the symbolwise ED fails completely in demodulating the received signal. The ED-MLSE performs roughly similar as TR-T with $M1$. This points out the superiority of TR with respect to ISI in general due to inherent CSI acquired by the reference pulse. Although the MLSE improves the performance of the ED significantly, it can not fully compensate for the information loss of the ED. The performance gap between analysis and simulation results for M1 and M3 arises from the cross-correlation terms which are ignored in the analysis. With growing number of samples in the integration window, the cross-terms approach their zero mean and therefore loose

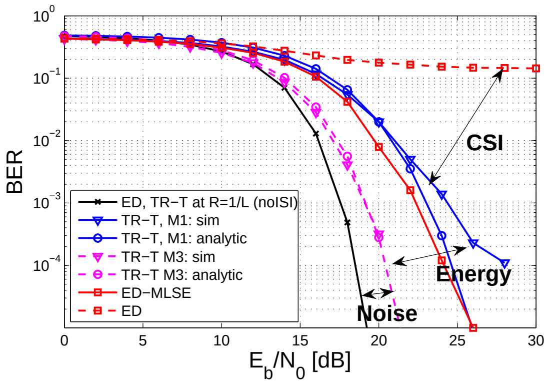

Fig. 6. BER of transmitted reference in case of moderate ISI with $D = N/3 = L/3$.

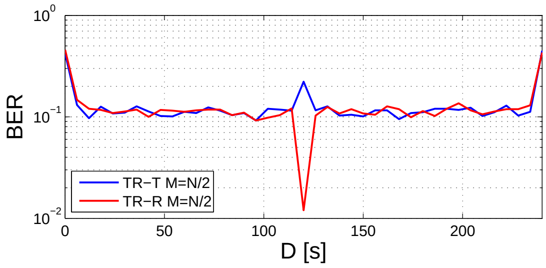

Fig. 7. BER of TR-T and TR-R in case of moderate ISI and fixed integration duration $M = N/2 = L/2$ as a function of delay D.

their impact on the results. Therefore, the gap decreases from M1 to M3. Due to the marginal impact of the cross-terms, integration over the whole frame M3 leads to the best performance. Hence, in case of $D \neq \frac{N}{2}$, it is more important to collect sufficient energy than avoiding ISI and aliasing terms. The performance gap between TR-T M3 and TR-T which operates at data rate R and avoids ISI is due to correlated noise terms in M3, which lead to noise enhancement.

Fig. 7 shows the BER performance of TR-T and TR-R as a function of the delay D. While frame and integration duration were fixed to $N = L$ and $M = N/2$, the delay was varied from $D = 0$ to $D = N = 240$. The SNR was set to $E_b/N_0 = 16$ dB . For $D \neq N/2$, the BER performances of TR-T and TR-R are similar and hardly depend on D. This is again because the instantaneous ISI terms approach their mean 0. It is apparent that $D = N/2$ is a special case, where the impact of ISI is strong. While TR-R fails completely, TR-T gains a lot from the special ISI structure. Hence, depending on the choice of TR-T or TR-R, $D = N/2$ is a worst or best case scenario. This is plotted again in Figure 8. The BER performance of TR-R and TR-T applying $D = N/2$ are compared to DPSK under average and peak power constraint. Contrary to TR-T, TR-R shows very promising performance and outperforms TR-T M3 and even TR-T at half the rate R. Due to the lack of repeated reference pulses, DPSK at data rate $\hat{R}$ encounters no ISI and with respect to average power is allowed to transmit twice the pulse energy as the corresponding UWB TR system, leading to $P_{e|\vec{h}} = \mathcal{Q}\left(\|\vec{h}\|^2/\sqrt{\|\vec{h}\|^2\sigma^2/2 + L\sigma^4/16}\right)$. This is clearly better than (31), which is confirmed by the results in Fig. 8. However results from [1], [5] show that in UWB systems the peak power and not the average power is often the limiting factor from a regulation and a design point of view. Normalizing the DPSK transmit signal to the same peak power as the UWB TR leads to a performance degradation making the UWB TR system preferable.

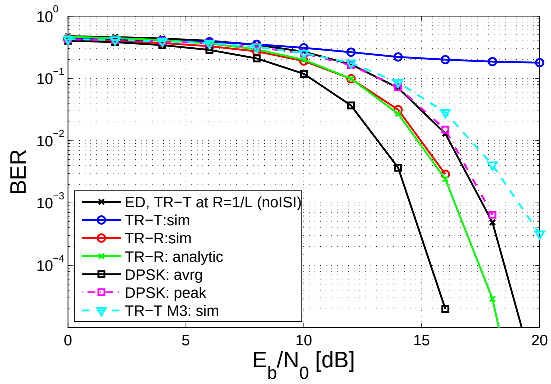

Fig. 8. BER performance for TR-T and TR-R with $D = N/2 = L/2$ and DPSK

V. Conclusions

The impact of moderate ISI on low complexity UWB TR schemes is analyzed. While TR and BPPM-ED show the same performance in absence of ISI, TR is much more robust to ISI due to the inherent CSI acquired by the reference pulse. In the general case $D \neq N/2$, the impact of ISI is marginal and BER performance depends mainly on the amount of collected signal energy. Therefore, TR-T and TR-R show similar performance. In the special case $D = N/2$ the impact of ISI is strong. While TR-T fails completely to demodulate the received signal, TR-R even shows performance gains in presence of ISI. This is possible as the specific ISI structure allows the receiver to collect the entire signal energy while integrating over a shorter time window. Also in absence of ISI, $D = N/2$ is a special case, where TR-T and TR-R lead to performance losses or gains, respectively, if integration is done over the whole frame.

VI. Acknowledgment

The authors would like to thank Jürg Schaub for his valuable inputs to this paper during his master thesis. The work presented in this paper was partially supported by the National Competence Center in Research on Mobile Information and Communication Systems (NCCR-MICS), a center supported by the Swiss National Science Foundation under grant number 5005-67322.

References

[1] F. Troesch, C. Steiner, T. Zasowski, and A. Wittneben, "Hardware aware optimization of an ultra low power UWB communication system," in *IEEE Int. Conf. Ultra-Wideband (ICUWB)*, Singapore City, Singapore, September 24 – 26, 2007.

[2] Q. Hieu and A.-J. Van Der Ven, "Resolving inter-frame interference in a tramsit-reference ultra-wideband communication system," in *Proc. ICASSP*, Toulouse, France, May 14 –19 2006.

[3] B. Sadler, J. Tang, and Z. Xu, "Performance analysis of b-bit digital receivers for TR-UWB systems with inter-pulse interference," *IEEE Trans. Wirel. Comm.*, vol. 6, no. 2, pp. 494–504, Feb. 2007.

[4] K. Witrisal, G. Leus, M. Pausini, and C. Krall, "Equivalent system model and equalization of differential impulse radio UWB systems," *IEEE J. Select. Areas Commun.*, vol. 23, no. 9, pp. 1851–1860, Sept. 2005.

[5] F. Troesch, F. Althaus, and A. Wittneben, "Modified pulse repetition coding boosting energy detector performance in low data rate systems," in *IEEE Int. Conf. Ultra-Wideband (ICU)*, Zurich, Switzerland, Sept. 5 – 8, 2005.

[6] F. Troesch and A. Wittneben, "MLSE post-detection for ISI mitigation and synchronization in UWB low complexity receivers," in *IEEE Veh. Tech. Conf.*, Dublin, Ireland, 2006.

[7] S. Dubouloz, B. Denis, S. De Rivaz, and L. Ouvry, "Performance analysis of LDR UWB non-coherent receivers in multipath environments," in *IEEE Int. Conf. Ultra-Wideband (ICU)*, Zurich, Switzerland, Sept. 5 – 8, 2005, pp. 491–496.